Luminescent Organic Radicals

DOI: 10.1002/ange.201407362

Luminescence, Stability, and Proton Response of an Open-Shell (3,5-Dichloro-4-pyridyl)bis(2,4,6-trichlorophenyl)methyl Radical**

Yohei Hattori, Tetsuro Kusamoto, and Hiroshi Nishihara**

Abstract: *A luminescent open-shell organic radical with high chemical stability was synthesized. (3,5-Dichloro-4-pyridyl)-bis(2,4,6-trichlorophenyl)methyl radical (PyBTM) was photoluminescent under various conditions. Fluorescence quantum yields of 0.03, 0.26, and 0.81 (the highest value reported for a stable organic radical) were obtained in chloroform, in poly(methyl methacrylate) film at room temperature, and in an EPA matrix (diethyl ether:isopentane:ethanol) at 77 K, respectively. The photostability of PyBTM is up to 115 times higher than that of the tris(2,4,6-trichlorophenyl)methyl radical, a previously reported luminescent radical. The pyridine moiety of PyBTM acts as a proton coordination site, thereby allowing for control of the electronic and optical properties of the radical by protonation and deprotonation.*

Luminescent molecules have been extensively studied for multiple applications in materials science, such as in organic light-emitting diodes[1] and chemical sensors.[2] While almost all known luminescent molecules are of closed-shell nature in the ground state, the characteristic luminescent properties of organic radicals with open-shell character have attracted interest recently.[3,4] Open-shell luminescent materials exhibit luminescence at long wavelengths without extended π-conjugated structures. Monoradicals (or triplet biradicals) display a spin-allowed fluorescent transition from the doublet (or triplet) lowest excited state to the doublet (or triplet) ground state. Unlike conventional closed-shell fluorescent molecules, the emission processes of monoradicals (or triplet biradicals) do not suffer from annihilation through the triplet state, such as by singlet–triplet intersystem crossing or charge recombination. A good fluorescence quantum yield (ϕ) and a high luminescence efficiency in electroluminescent devices would therefore be expected for these systems.[5]

To date, several problems have hindered investigation of the photofunctions of luminescent organic radicals, including: 1) there are relatively few examples of luminescent organic radicals, and 2) the molecules degrade upon photoexcitation.[6] Perchlorotriphenyl methyl radical (PTM), a rare example of a fluorescent organic stable radical (λ_{em} = 605 nm, $\phi = 0.015$ in CCl_4), is chemically stable under ambient conditions, but decomposes under irradiation with light to yield the nonfluorescent perchloro-9-phenylfluorenyl radical with a quantum efficiency of 0.3.[6a] Decomposition was also found in other fluorescent organic radicals,[4,6b] including the tris(2,4,6-trichlorophenyl)methyl radical (TTM)[7] investigated herein. Establishing a method for improving the photostability will expand the scope of luminescent organic radicals; an interplay between the luminescent, magnetic, and electronic properties is expected to provide magnetic (spin), electronic, and photoresponsive molecular devices.

We have prepared a novel luminescent stable radical, (3,5-dichloro-4-pyridyl)bis(2,4,6-trichlorophenyl)methyl radical (PyBTM, Figure 1), with a unique molecular design. A

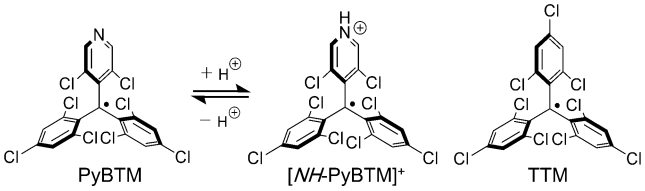

Figure 1. Structure of PyBTM, protonated PyBTM ([*NH*-PyBTM]$^+$), and TTM.

pyridine ring was incorporated into the TTM skeleton. The substitution is expected to lower the energies of the frontier molecular orbitals on the TTM skeleton owing to the greater effective nuclear charge (electronegativity) of the nitrogen atom than that of the carbon atom, thus leading to enhanced photostability. Herein, we discuss the electronic structure, optical properties, and stability of PyBTM. The nitrogen atom on the pyridyl group allows for a reversible proton response, which tunes the properties of PyBTM.

PyBTM was prepared in 3 steps from commercially available reagents in 61% yield[8,9] and characterized by FTIR spectroscopy, high-resolution ESI-TOF mass spectrometry, and elemental analysis. The existence of $S = 1/2$ spin on one PyBTM molecule was confirmed using electron spin resonance (ESR) spectroscopy (Supporting Information). The single-crystal X-ray structure of PyBTM shows that the methyl carbon atom C1, shielded sterically by 6 chlorine atoms, is sp^2 hybridized: carbon atom C1 and the three carbon

[*] Y. Hattori, Dr. T. Kusamoto, Prof. Dr. H. Nishihara
Department of Chemistry, School of Science
The University of Tokyo
7-3-1 Hongo, Bunkyo-ku, Tokyo, 113-0033 (Japan)
E-mail: kusamoto@chem.s.u-tokyo.ac.jp
nisihara@chem.s.u-tokyo.ac.jp
Homepage: http://www.chem.s.u-tokyo.ac.jp/users/inorg/new_en/index.html

[**] We are grateful to Dr. Reizo Kato at RIKEN for his kind provision of facilities and laboratory equipment. This work was supported financially by Grants-in-Aid from MEXT of Japan (Grants 26220801, 24750142, and 21108002; area 2107 (coordination programming)), and MERIT (Material Education program for the future leaders in Research, Industry, and Technology) in the MEXT Leading Graduate School Doctoral Program.

Supporting information for this article is available on the WWW under http://dx.doi.org/10.1002/anie.201407362.

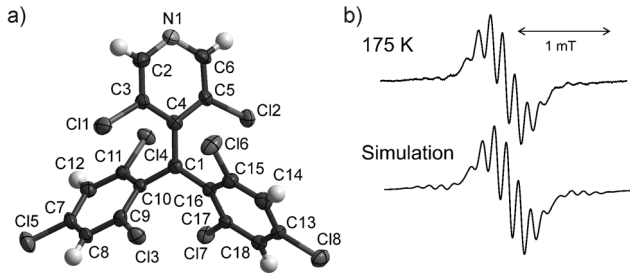

Figure 2. a) Molecular structure of crystalline PyBTM with thermal ellipsoids set at 50% probability. b) ESR spectrum of PyBTM in CH_2Cl_2 solution at 175 K (top) and computer simulation (bottom).

atoms bonded to C1 (C4, C10, and C16) lie in one plane (Figure 2a; Tables S1 and S2 in the Supporting Information).[10] PyBTM showed high chemical stability under ambient conditions (Supporting Information).

The spin-density distribution of PyBTM was estimated using the ESR spectrum recorded in CH_2Cl_2 at 175 K (Figure 2b). The spectra was reproduced by computer simulation by considering the hyperfine coupling with ^1H, ^{14}N, and ^{13}C atoms, the constants of which are shown in Table S3 in the Supporting Information. The spin density is distributed on the central C atom and also on the phenyl and pyridyl moieties; the distribution is reproduced by DFT calculations (Figure S1).

The electronic structure of PyBTM was estimated by DFT calculations (Figure 3). The results show that the SOMO (129α) is delocalized onto the aromatic rings (SOMO = singly occupied molecular orbital). The energy of the SOMO of PyBTM (−5.96 eV) is lower than the SOMO of TTM (137α, −5.75 eV in Figure S2) by 0.21 eV, and the energy of the lowest unoccupied β orbital of PyBTM (129β, −3.62 eV) is lower than that of TTM (137β, −3.44 eV) by 0.18 eV. These positive shifts correspond to the shifts of the reversible reduction potential $E^{0\prime}_{(red)}$ and the irreversible oxidation peak $E_{p(ox)}$ in the cyclic voltammogram ($E^{0\prime}_{(red)} = -0.74$ V and $E_{p(ox)} = 1.04$ V versus ferrocenium/ferrocene for PyBTM; $E^{0\prime}_{(red)} = -0.99$ V and $E_{p(ox)} = 0.80$ V for TTM; Figure S3). The

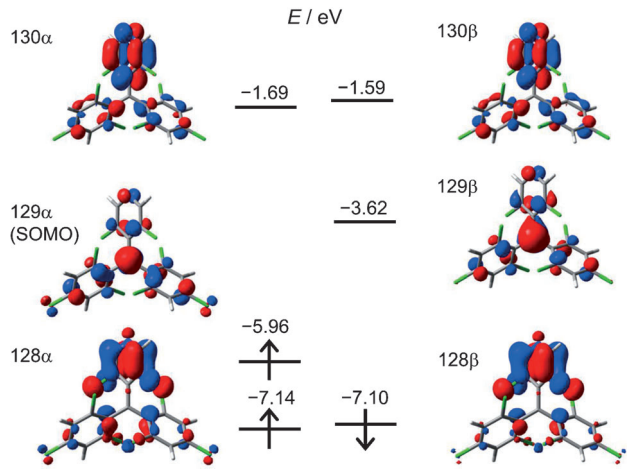

Figure 3. Frontier orbitals of PyBTM calculated using DFT methods (UB3LYP/6-31G(d)).

DFT calculations and cyclic voltammetry confirm that the introduction of the pyridine moiety lowers the energies of the frontier molecular orbitals.

The UV/Vis absorption spectrum of PyBTM in CH_2Cl_2 (Figure 4) displayed a weak visible absorption band that tails

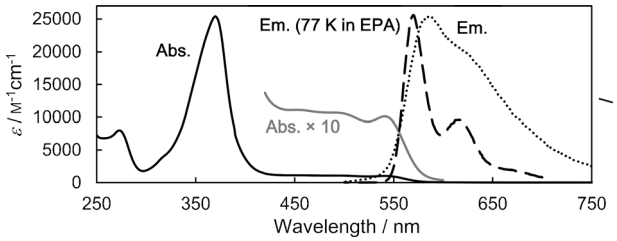

Figure 4. Absorption (solid line) and corrected emission spectra (dotted line) of PyBTM in CH_2Cl_2 at room temperature, and corrected emission spectra at 77 K in EPA matrix (dashed line) for PyBTM. Enlarged portion of absorption spectra (10 fold) are shown from $\lambda = 420$ nm to 600 nm (gray line). I = intensity.

off beyond $\lambda = 600$ nm ($\lambda_{max} = 541$ nm, $\varepsilon = 1.01 \times 10^3\,M^{-1}cm^{-1}$; where ε is the molar extinction coefficient), and a strong near-UV absorption band ($\lambda_{max} = 370$ nm, $\varepsilon = 2.54 \times 10^4\,M^{-1}cm^{-1}$). Time-dependent DFT calculations (TDDFT) suggested that the band at $\lambda_{max} = 541$ nm can be assigned to the transition mainly from 128β (π orbital of pyridine) to 129β (lowest unoccupied spin orbital; oscillator strength $f = 0.019$), to form a lowest excited state, whereas the band at $\lambda_{max} = 370$ nm is assigned to the transition mainly from 129α (SOMO) to 130α and 131α (antibonding π* orbitals) with a greater oscillator strength ($f = 0.120$, 0.151). The agreement of the relative wavelength and oscillator strength with the experimental absorption spectra supports the orbital assignment. A TDDFT calculation of TTM gave similar results (Figure S4).

The fluorescence spectra of PyBTM in CH_2Cl_2 upon excitation at $\lambda_{exc} = 370$ nm (Figure 4) showed a band with an emission maximum at $\lambda = 585$ nm. The shape of the excitation spectrum was similar to that of the absorption spectrum (Figure S5). The excited-state luminescence lifetime (τ) was 6.4 ± 0.2 ns in dichloromethane with a single-exponential decay, similar to those of TTM ($\tau = 7.0 \pm 0.2$ ns) and PTM ($\tau = 7$ ns),[6a] supporting the assignment of the emission as fluorescent in nature.

The photophysical processes of PyBTM are rationalized as follows. The excitation with light at $\lambda = 370$ nm mainly induces 129α→130α and 129α→131α electronic transitions centered on the α spins, leading to the formation of doublet $D_{\alpha 1}$ and $D_{\alpha 2}$ excited states (Figure S6). These excited states relax efficiently to the lowest excited state $D_{\beta 1}$ (D_1), which is represented by the β-spin excitation (128β→129β). Such rearrangement of spins in the excited states (from α-spin-centered excited states to β-spin-centered excited states) is not considered in the emission process of conventional closed-shell fluorescent molecules. The photophysical processes are spin-allowed in nature and follow Kasha's rule. The $D_{\beta 1}$ state eventually relaxes to the ground state (D_0) with fluorescent emission. It is noted that the lowest excited quartet state (Q_1, 128β→130α) is higher in energy than the

D_x excited states, and thus the Q_1 state cannot be an annihilation path.

PyBTM displayed similarly shaped absorption and emission bands in cyclohexane, chloroform, dichloromethane, acetone, acetonitrile, ethanol, and methanol. The absolute photoluminescence quantum yields were typically 1–3% with PyBTM appearing as luminescent as TTM (Table S4). The absorption and emission intensities were temperature-dependent (Figures S7 and S8), and strong luminescence was detected at low temperature in rigid solvents. PyBTM was luminescent at 77 K with excellent absolute photoluminescence quantum yields of 0.81 in EPA (diethyl ether:isopentane:ethanol 5:5:2 v/v) and 0.71 in a mixture of ethanol and methanol (1:1 v/v). The quantum yield of 0.81 is the highest value reported for stable organic radicals. This high quantum yield results from the suppression of the molecular vibrations that promote nonradiative decay.

The results prompted us to disperse the PyBTM molecules in a poly(methyl methacrylate) (PMMA) film. The rigid polymer chains should suppress the molecular motion of the PyBTM. The film showed luminescence with $\phi = 0.26$ at room temperature under irradiation with light ($\lambda = 370$ nm). The encapsulation of PyBTM in a PMMA matrix resulted in a quantum yield that is approximately ten times higher than that in solution.

The improvement of the photostability of luminescent organic radicals is an important issue in the development of luminescent paramagnetic molecular-based materials. The photostability of PyBTM was evaluated and compared with that of TTM (Figure 5a). When acetone solutions of PyBTM and TTM (approximately 1×10^{-5} M) were irradiated at $\lambda =$ 370 nm, the decay of the fluorescence intensity of PyBTM ($1/t_{1/2(\mathrm{PyBTM})}$) was 115 times smaller than that of TTM ($1/t_{1/2(\mathrm{TTM})}$; Figure 5b). In other aprotic solvents, PyBTM was 45 to 71 times more stable than TTM (Figure S9). TTM was also shown to undergo efficient photolysis even under natural light. The introduction of the pyridyl group therefore enhances the photostability of the PyBTM radical. This results from the lowered energies of the molecular orbitals involved in the luminescence process, as shown by the cyclic voltammograms and the DFT calculations.

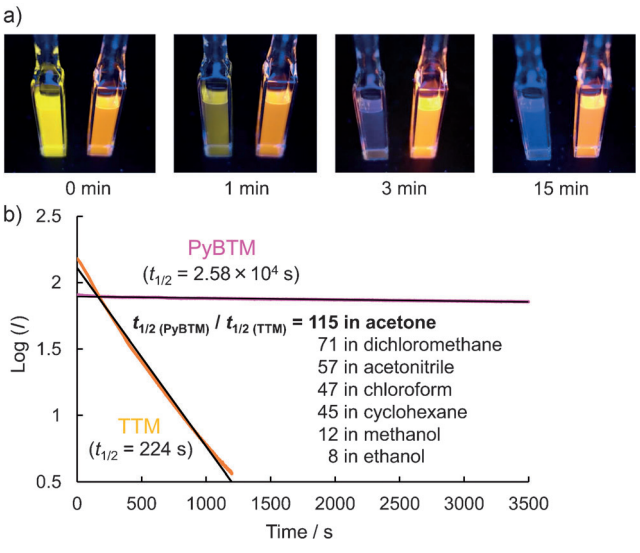

Figure 5. a) Photographs of TTM (left cuvette in each image) and PyBTM (right cuvette) solutions (2.5×10^{-4} M) in acetone under irradiation with UV light at $\lambda = 370$ nm recorded at different time intervals, showing the emission decay with time. b) Plots showing the emission decay of PyBTM and TTM in acetone under continuous excitation with light at $\lambda = 370$ nm. Ratios of half-lives ($t_{1/2}$) in various solvents are given.

We next attempted to control the properties of PyBTM by a protonation–deprotonation reaction on the N atom of the pyridyl group. The reversible response of the molecule towards protonation was shown using UV/Vis absorption spectroscopy by an acid–base titration (Figure S10). Protonation significantly influences the luminescence properties, with a decrease of fluorescence intensity detected upon addition of the acid (Figure S11). Protonation of PyBTM at the nitrogen atom was supported by the single-crystal X-ray structure of [*NH*-PyBTMH]·BF_4·H_2O (Figure S12, Table S1).[10] The redox properties were also modulated by reversible protonation and deprotonation, demonstrating the drastic change of the electron-accepting ability of the molecule upon protonation (Figure S13).

In conclusion, a new luminescent stable organic radical PyBTM showed a significantly greater photostability than previously reported for luminescent organic radicals. The stability is attributed to the lower energy of the frontier orbitals resulting from the introduction of a nitrogen atom. PyBTM exhibited a high luminescence quantum yield in solvent glass at 77 K and a moderate quantum yield in PMMA at room temperature. Reversible protonation at the pyridine N atom can switch the properties of PyBTM. Metal complexes with coordinated PyBTM molecules are also expected to show interesting luminescence properties and are currently under investigation.

Received: July 18, 2014
Revised: August 24, 2014
Published online: September 11, 2014

Keywords: density functional calculations · luminescence · photostability · protonation · radicals

[1] a) Y. Sun, N. C. Giebink, H. Kanno, B. Ma, M. E. Thompson, S. R. Forrest, *Nature* **2006**, *440*, 908–912; b) H. Uoyama, K. Goushi, K. Shizu, H. Nomura, C. Adachi, *Nature* **2012**, *492*, 234–238.

[2] a) J. F. Callan, A. P. de Silva, D. C. Magri, *Tetrahedron* **2005**, *61*, 8551–8588; b) X. Chen, Y. Zhou, X. Peng, J. Yoon, *Chem. Soc. Rev.* **2010**, *39*, 2120–2135.

[3] a) V. Gamero, D. Velasco, S. Latorre, F. López-Calahorra, E. Brillas, L. Juliá, *Tetrahedron Lett.* **2006**, *47*, 2305–2309; b) D. Velasco, S. Castellanos, M. López, F. López-Calahorra, E. Brillas, L. Juliá, *J. Org. Chem.* **2007**, *72*, 7523–7532; c) L. Fajalí, R. Papoular, M. Reig, E. Brillas, J. L. Jorda, O. Vallocorba, J. Rius, D. Velasco, L. Juliá, *J. Org. Chem.* **2014**, *79*, 1771–1777.

[4] A. Heckmann, S. Dümmler, J. Pauli, M. Margraf, J. Köhler, D. Stich, C. Lambert, I. Fischer, U. Resch-Genger, *J. Phys. Chem. C* **2009**, *113*, 20958–20966.

[5] H. Namai, H. Ikeda, Y. Hoshi, N. Kato, Y. Morishita, K. Mizuno, *J. Am. Chem. Soc.* **2007**, *129*, 9032 – 9036.
[6] a) M. A. Fox, E. Gaillard, C.-C. Chen, *J. Am. Chem. Soc.* **1987**, *109*, 7088 – 7094; b) S. R. Ruberu, M. A. Fox, *J. Phys. Chem.* **1993**, *97*, 143 – 149.
[7] O. Armet, J. Veciana, C. Rovira, J. Riera, J. Casteñer, E. Molins, J. Rius, C. Miravitlles, S. Olivella, J. Brichfeus, *J. Phys. Chem.* **1987**, *91*, 5608 – 5616.
[8] D. A. Klumpp, Y. Zhang, P. J. Kindelin, S. Lau, *Tetrahedron* **2006**, *62*, 5915 – 5921.
[9] L. Juliá, M. Ballester, J. Riera, J. Casteñer, J. L. Ortin, C. Onrubia, *J. Org. Chem.* **1988**, *53*, 1267 – 1273.
[10] CCDC-1006484 (PyBTM), and 1006485 ([*NH*-PyBTMH]·BF_4·H_2O) contain the supplementary crystallographic data for this paper. These data can be obtained free of charge from The Cambridge Crystallographic Data Centre via www.ccdc.cam.ac.uk/data_request/cif.